Journal of Colloid and Interface Science 490 (2017) 462–477

Contents lists available at ScienceDirect

Journal of Colloid and Interface Science

journal homepage: www.elsevier.com/locate/jcis

Regular Article

Tuning particle geometry of chemically anisotropic dumbbell-shaped colloids

Bas G.P. van Ravensteijn [1], Willem K. Kegel

Van't Hoff Laboratory for Physical and Colloid Chemistry, Debye Institute for NanoMaterials Science, Utrecht University, Padualaan 8, 3584 CH Utrecht, The Netherlands

GRAPHICAL ABSTRACT

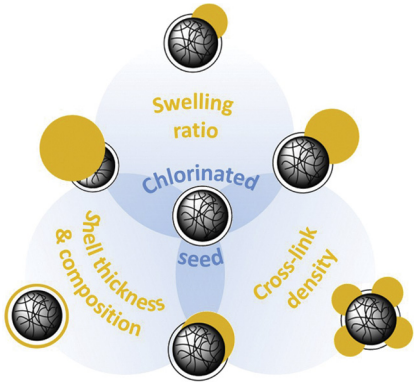

ARTICLE INFO

Article history:
Received 7 September 2016
Revised 10 November 2016
Accepted 14 November 2016
Available online 15 November 2016

Keywords:
Dumbbell-shaped colloids
Emulsion-based synthesis
Chemically anisotropic particles

ABSTRACT

Chemically anisotropic dumbbell-shaped colloids are prepared starting from cross-linked polymer seed particles coated with a chlorinated outer layer. These chlorinated seeds are swollen with monomer. Subsequently, a liquid protrusion is formed on the surface of the seed particle by phase separation between the monomer and the swollen polymer network. Solidification of these liquid lobes by polymerization leads to the desired dumbbell-shaped colloids. The chlorine groups remain confined on the seed lobe of the particles, ensuring chemical anisotropy of the resulting particles. Exploiting the asymmetric distribution of the chemically reactive surface chlorine groups allows for site-specific surface modifications.

Here we show that the geometry of the resulting chemically anisotropic dumbbells can be systematically tuned by a number of experimental parameters including the volume of styrene by which the seeds are swollen, the cross-link density of the chlorinated seeds and chemical composition/thickness of the chlorinated coating deposited on the seed particles. Being able to control the particle geometry, and therefore the Janus balance of these chemically anisotropic particles, provides a promising starting point for the synthesis of sophisticated building blocks for future (self-assembly) studies.

1. Introduction

Emulsion-based syntheses of anisotropic colloids are promising routes towards the large scale production of such particles. Several authors reported on the preparation of dumbbell-shaped colloids

[1] Present address: Department of Chemical Engineering, University of California Santa Barbara, Santa Barbara, CA 93105, USA.

E-mail addresses: bas.van.ravensteijn@gmail.com (B.G.P. van Ravensteijn), w.k.kegel@uu.nl (W.K. Kegel)

http://dx.doi.org/10.1016/j.jcis.2016.11.045
0021-9797/

using this type of syntheses leading to a variety of particles where the particle shape and size can be tuned in a controlled fashion [1–13].

Sheu et al. pioneered this field and demonstrated that raising the temperature of monomer-swollen cross-linked polystyrene particles causes the monomer to phase-separate from the seed particle as a liquid protrusion. Subsequent polymerization of the monomer composed protrusions yields anisotropic dumbbell-shaped colloids [14,15]. A thermodynamic model was provided that accounts for swelling of polymer networks with hydrophobic monomers with low water solubility, such as styrene. The free energy of monomer within the network ($\Delta\overline{G}_{m,p}$) relative to the free energy of monomer residing in a droplet in the aqueous phase can be approximated by the sum of the free energy of mixing the monomer with the polymer ($\Delta\overline{G}_{m}$) [16,17], the elastic energy resulting from stretching the cross-linked polymer network in the seed particles ($\Delta\overline{G}_{el}$) [18], and the surface tension of the particle with the aqueous phase ($\Delta\overline{G}_{t}$) [19].

$$\begin{aligned}\Delta\overline{G}_{m,p} &= \Delta\overline{G}_{m} + \Delta\overline{G}_{el} + \Delta\overline{G}_{t} \\ &= RT[ln(1-\phi_p) + \phi_p + \chi_{m,p}\phi_p^2] + RTNV_m(\phi_p^{1/3} - \phi_p/2) + \frac{2V_m\gamma}{r}\end{aligned} \quad (1)$$

Here, R is the ideal gas constant, T is the temperature, ϕ_p is the volume fraction of polymer in the swollen seed particle, $\chi_{m,p}$ is the monomer-polymer interaction parameter, N is the effective number of chains in the network per unit volume, V_m is the monomer molar volume, γ is the interfacial tension between the particle and water, and r is the radius of the swollen seed particle.

From this equation we learn that $\Delta\overline{G}_{el}$ and $\Delta\overline{G}_{t}$ restrict the swelling process (positive contribution to $\Delta\overline{G}_{m,p}$) while $\Delta\overline{G}_{m}$ promotes swelling by a negative contribution to $\Delta\overline{G}_{m,p}$. Intuitively this is easy to understand since it is energetically unfavorable for a cross-linked polymer network to expand due to build-up of elastic stresses. Furthermore, swelling the particle leads to a larger interfacial area between the particle surface and the continuous phase, hence a higher surface free energy. On the other hand, transporting hydrophobic monomer from the aqueous phase to the hydrophobic interior of the seed particles is energetically favorable, thus promoting the swelling process. Swelling proceeds until the monomer inside the polymer network is in coexistence with monomer in the aqueous phase, *i.e.*, the sum of all three contributions equals zero. At this point the monomer swollen particles reach their equilibrium size.

In order to form a liquid protrusion, the monomer needs to phase separate from the swollen particles. This phase separation is driven by relaxation of the polymer network. Upon relaxation an elastic-retractile force is generated which forces out the monomer used to swell the particles. This relaxation is in principle a spontaneous process [13], although the rate of monomer expulsion can be slow. This process can be sped up considerably if the swollen particles are heated [14,15]. Heating causes an increase in the elastic free energy ($\Delta\overline{G}_{el}$) leading to a positive value of $\Delta\overline{G}_{m,p}$, *i.e.*, the system is in an unfavorable state, promoting the phase separation between the monomer and the polymer network. Expulsion of the monomer continues until a new coexisting condition is reached. Sheu et al. reported that for large particles initial phase separation yielded a small liquid protrusion. The protrusion grows during polymerization of this additional lobe, since monomer is continuously withdrawn from the swollen seed particle driven by an imbalance of the chemical potential [14,15]. The swollen seed particle acts therefore as a monomer reservoir and consequently, protrusion formation follows a nucleation and growth type of mechanism (Scheme 1, blue bottom route). More recently, dumbbell formation was suggested to proceed via one discrete phase separation step, resulting in colloids that carry large liquid protrusions on their surface (Scheme 1, green top route) [1,2]. Both mechanisms lead to the same well-defined dumbbell-shaped colloids.

The work of Sheu et al. focused on micron-sized seed particles (2–8 μm diameter). It was concluded that the degree of phase separation increases with increasing dimensions of the seeds. Using particles with a diameter on the order of 500 nm did not result in the formation of a protrusion. The absence of protrusion formation for small seeds can be easily rationalized if the third contribution in Eq. (1) is considered. This so-called Morton equation states that the interfacial pressure at the swollen particle/water interface is inversely proportional to the radius of the particles. If the particle size becomes small enough, a point is reached where the sum of the interfacial and the mixing force exceed the thermo-induced elastic-retractile force. In this situation, no phase separation will occur and the monomer is trapped inside the polymer network. Inducing polymerization of the swelling monomer in this situation obviously yields larger spherical particles, instead of the desired dumbbells.

However, Mock et al. circumvented the absence of phase separation for colloidal particles with sizes on the order of 200–500 nm [20]. They realized that the contribution of $\Delta\overline{G}_{t}$ is actually determined by the ratio between the surface tension and the particle radius. By applying hydrophilic coatings of poly(vinyl acetate) or poly(acrylic acid), the surface tension between the swollen particle/water interface is significantly lowered. This results in a decreasing contribution of $\Delta\overline{G}_{t}$ and hence promotes the tendency for monomer phase separation. An additional beneficial effect of the hydrophilic coatings is that the expelled monomer only partially wets the surface of the seed particle. This enhances the formation of a well-separated monomer bulge on the seeds with a controlled contact angle, leading to more pronounced shape-anisotropy of the resulting dumbbells.

Recently, we showed that the procedure of Mock et al. can be extended to particles that contain coatings which are not only hydrophilic, but also reactive towards subsequent surface modification reactions. We coated particles with a thin, cross-linked layer of 4-vinylbenzyl chloride (VBC), yielding particles with reactive benzyl chloride moieties on their surface. We showed that upon protrusion formation, these reactive chemical handles remained confined on the seed lobes, generating shape and chemically anisotropic particles in the colloidal regime [5]. The localized benzyl chloride moieties allow for further site-specific surface modification reaction, *e.g.*, using click chemistry or controlled polymer grafting, to tune the (physical) patch characteristics on demand [5,21].

Here, we explore which particle geometries are accessible using the chlorinated seed particles and how the seed properties influence the protrusion formation step. Being able to tune the shape of these chemically anisotropic colloids is an important step towards using these particles with functionalized patches in, for example, self-assembly studies where the final super-structure heavily depends on the geometry of the employed building blocks [22–28].

2. Experimental section

2.1. Materials

Styrene (St, *ReagentPlus*, contains 4-*tert*-butylcatechol as stabilizer, ⩾99%), divinylbenzene (DVB, 55% mixture of isomers, tech. grade, ⩽1500 ppm 4-*tert*-butylcatechol as inhibitor), 4-vinylbenzyl chloride (VBC, ⩾90%, tech. grade, 0.05% 4-*tert*-butylcatechol and 0.05% nitro-paraffin as stabilizer) and *N*,*N*-dimethyl-

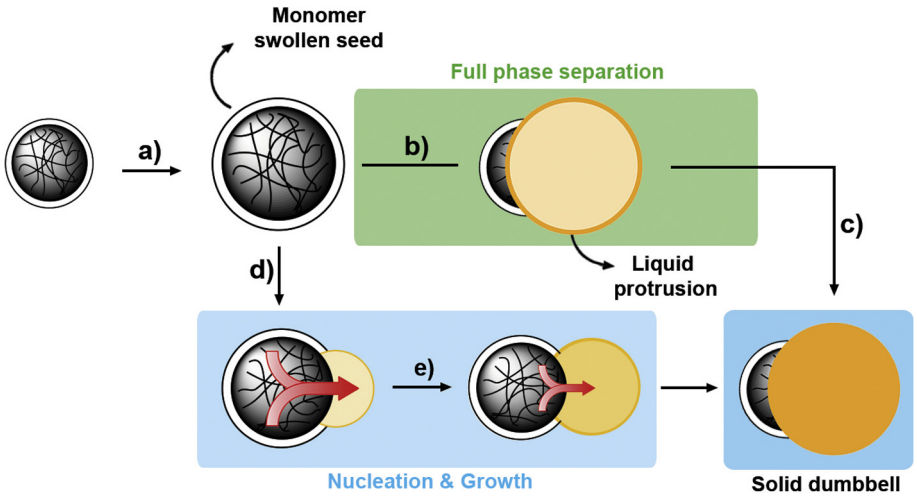

Scheme 1. Schematic representation of the reported mechanisms for protrusion formation from monomer swollen seed particles. Both mechanisms start by swelling a seed particle with monomer (step a). According to the *full phase separation* mechanism, highlighted in green (top), all the monomer phase separates (nearly) simultaneously, leading to the formation of large liquid protrusions. Polymerization of these liquid lobes yields fully solid, well-defined dumbbell-shaped particles. Alternatively, the initial phase separation generates only a small liquid protrusion (step d). After initiating polymerization of the protrusion, monomer is consumed leading to the formation of a monomer flow from the monomer swollen seed to the protrusion (red arrows, step e). The supply of monomer from the seeds continues until the monomer is depleted. Polymerization proceeds in the newly formed lobe until maximum conversion is reached. Similar dumbbell-shaped colloids are obtained via this *nucleation and growth* type of mechanism (highlighted in blue, bottom).

formamide (DMF, *ReagentPlus*, ⩾99%) were obtained from Sigma-Aldrich. Hydroquinone (*puriss.*, ⩾99.5%) was purchased from Riedel-de Haën. Sodium dodecyl sulfate (SDS, 99%) from BDH was used. Potassium persulfate (KPS, >99% for analysis), sodium bisulfite ($NaHSO_3$, ACS reagent, mixture of $NaHSO_3$ and $Na_2S_2O_5$), azobis(isobutyronitrile) (AIBN, 98%) and tetrahydrofuran (THF, 99.6%, ACS reagent, stabilized with BHT) were purchased from Acros Organics. All chemicals were used as received. The water used for all syntheses was purified using a Milli-Q water purification system (resistivity = 18.2 MΩ cm at 25 °C).

2.2. Synthesis of cross-linked polystyrene colloids (CPs)

Typically, cross-linked polystyrene particles (CPs) were synthesized using a standard emulsion polymerization method described in literature [1,5]. A 500 mL round-bottom flask equipped with magnetic stir bar was placed in an oil bath at 80 °C. Water (200 mL) was charged into the reactor and allowed to reach the bath temperature. Styrene (23 mL, 0.2 mol), DVB (0.7 mL, 5 mmol), and SDS (0.25 g, 0.9 mmol) dissolved in water (50 mL) were added. The complete mixture was allowed to heat up to the temperature of the bath. Finally, the addition of KPS (0.39 g, 1.4 mmol dissolved in 37.5 mL of water) initiated the polymerization. The reaction was allowed to continue for 24 h at 80 °C. The resulting latex had a solid content of 7% (measured gravimetrically). The obtained particles had a radius of 125 nm with a polydispersity of 3.8% as determined with transmission electron microscopy (TEM). Details on this analysis can be found in the Characterization section. A hydrodynamic radius of 135 nm and polydispersity index (PDI) of 0.030 were measured using dynamic light scattering (DLS).

This standard synthesis procedure yielded particles with a cross-link density of 3%. The cross-link density of these seed particles was varied by changing the ratio of DVB and styrene in the monomer feed. Particles containing cross-link densities ranging from 1% to 18% were prepared (see Supporting Information S1, Table S1).

2.3. Synthesis of (chlorinated) core-shell colloids (CPs-Cl)

The previously synthesized particles (CPs) were used as seeds in the second step, in which chlorine groups were introduced at the colloidal surface [5]. Crude seed dispersion (25 mL, solid content = 7%) and water (10 mL) were introduced into a 50 mL round-bottom flask equipped with a magnetic stir bar. The mixture was degassed with nitrogen for 30 min. VBC (1 mL, 6.6 mmol premixed with DVB, 20 μL, 0.15 mmol) was injected under inert atmosphere. The seeds were swollen for 1 h at 30 °C, after which the temperature was raised to 60 °C. When this temperature was reached, an initiator solution containing KPS (0.04 g, 0.15 mmol) and sodium bisulfite (0.03 g, 0.29 mmol) dissolved in water (2.5 mL) was injected. The reaction was allowed to run for 4 h. The particles were washed with ethanol and water by centrifugation and redispersion cycles. After the final centrifugation step, the particles were redispersed in water. The solid content of the resulting dispersion was adjusted to 5%. This procedure yielded particles with a radius of 155 nm and polydispersity of 4.4% as measured using TEM. A hydrodynamic radius of 170 nm and PDI of 0.029 were measured with DLS. The presence of the chlorine groups was confirmed using Fourier transform infrared spectroscopy (FT-IR, 1266 cm^{-1}) and X-ray photoelectron spectroscopy (XPS, 200 and 270 eV) [5,29,30].

Variations on this synthesis procedure to tune the shell thickness and composition were conducted. The shell thickness was systematically controlled by variation of the volume of VBC which was added to a fixed volume of crude CPs dispersion. For all shell formation reactions, the added VBC contained DVB to ensure the formed shells were cross-linked. Unless stated otherwise, the shells were cross-linked with equal density as the cores onto which the chlorinated layer was deposited. Monomer volumes and resulting shell thicknesses are listed in Supporting Information S2, Table S2.

The shell composition was varied by growing shells around CPs particles with a cross-link density of 3% using mixtures of styrene and VBC as monomer feed. The percentages of VBC in the monomer feed ranged from 0 to 100 vol%. A shell cross-link density of 3% was used for all compositions. Relevant properties of the obtained core-shell particles are listed in Supporting Information S2, Table S2.

2.4. Procedure for the synthesis of anisotropic particles based on chlorinated seeds

Typically, the spherical chlorinated seed particles were converted to anisotropic colloids using the method described in Refs.

[1,2,5]. SDS (42 mg, 0.15 mmol) was introduced into a 25 mL elongated reaction tube containing a magnetic stir bar. To this tube a dispersion containing the chlorinated seeds (1.25 mL, solid content = 5%) and water (1.25 mL) were added. The particles were swollen with styrene or mixtures of styrene and DVB for 48 h. The swelling ratio, here defined as the mass of added monomer divided by the total mass of polymer in the seed dispersion, was varied by the total volume of the added monomer (mixture). After the swelling period, the dispersion was heated at 80 °C for 2 h, causing the formation of a liquid protrusion at the surface of the seed particles. After this 2 h heating period, the mixture was allowed to cool down to room temperature. To polymerize the formed liquid protrusions, AIBN (2.4 mg, 15 μmol) dissolved in styrene (115 μL, 1 mmol) was added, as well as a hydroquinone solution (0.25 mL, 46 mg, 0.4 mmol in 50 mL of water). Hydroquinone was added to suppress polymerization in the aqueous phase. The polymerization was allowed to continue for 24 h at 80 °C. The resulting particles were washed with water using centrifugation and redispersion cycles to remove unwanted aggregates and secondary nuclei. The washed dispersion had a solid content of 1%.

Variations on this synthesis procedure can be found in the Supporting Information (Tables S1 and S2) where the swelling ratio, cross-link density of the seed/protrusion, SDS concentration in the reaction mixtures and (chemical) properties of the seeds particles were varied to investigate the influence of these parameters on the resulting particle shape.

2.5. Characterization

Transmission electron microscopy (TEM) images were taken with a Philips Tecnai10 electron microscope operating at 100 kV. Bright field images were recorded using a SIS Megaview II CCD camera. The samples were prepared by drying a drop of diluted aqueous particle dispersion on top of Formvar (R1202 Agar Scientific) coated copper grids (square 300 mesh, G2300C Agar Scientific). Images were taken at different spots on a single TEM grid to ensure the recorded images reflect particles found in the whole population. Analysis of the recorded images was performed using *iTEM* software. The radii of spherical particles or individual lobes of dumbbell-shaped particles were obtained by drawing circles around the contours of well-separated colloids. These circles were constructed by the *iTEM* software after selecting three points on the edge of an individual particle. In case of dumbbell-shaped particles, higher order patchy particles were omitted from this analysis, since we were interested in the size and dispersity of the individual lobes of these particles only. Polydispersity percentages from TEM analysis were obtained by manually counting 100–200 individual particles from different TEM images. From a distribution of diameters the percentages were obtained by dividing the standard deviation of the distribution by its arithmetic mean and multiplying this fraction by 100%.

Infrared (IR) spectra were obtained using a PerkinElmer Frontier FT-IR/FIR spectrometer. The attenuated total reflectance (ATR) mode was used. All measurements were performed on powders obtained by drying the corresponding particle dispersion.

Dynamic light scattering (DLS) and electrophoretic mobility measurements were performed using a Malvern Zetasizer Nano ZS instrument using highly diluted aqueous dispersions at 25 °C. The DLS measurements were taken in seven runs of 15 individual measurements in backscatter mode (173°). Disposable polystyrene cuvettes were used. The sizes of the colloids are reported as *Z*-average diameters and their corresponding polydispersity index (PDI). These values were obtained by using the cumulant method as described in Ref. [31].

For the electrophoretic mobility measurements, seven runs of at least 50 individual measurements were conducted to obtain a statistically reliable zeta (ζ) potential. Electrophoretic mobilities were measured in Milli-Q water using disposable folded capillary sample cells. The Hückel limit of the Henry equation was used to convert the measured electrophoretic mobilities to ζ potentials [32].

3. Results and discussion

3.1. General dumbbell-formation procedure

The general experimental procedure to prepare chemically anisotropic dumbbells consists of four synthesis steps, as schematically depicted in Scheme 2. Firstly, a conventional emulsion polymerization is conducted to prepare monodisperse, cross-linked polystyrene seed particles (Scheme 2, step a). Subsequently, these seeds are coated with a slightly hydrophilic poly(vinylbenzyl chloride) (p(VBC)) layer by means of a seeded emulsion polymerization (Scheme 2, step b). In the third step, the spherical chlorinated seeds are converted into anisotropic particles via the introduction of a liquid protrusion (Scheme 2, step c). To achieve this symmetry breaking, the chlorinated seeds are swollen with monomer. To facilitate the swelling process, surfactants are added. Monomer-swollen micelles act as transport agents for the hydrophobic monomer during transport through the aqueous continuous phase from large monomer droplets to the interior of the chlorinated particles. As discussed in the Introduction, monomer phase separates from the obtained monomer-swollen particles, resulting in the formation of a liquid protrusion residing on the surface of the chlorinated seed. At this stage, the presence of surfactants in the reaction mixtures is also beneficial, since the amphiphiles lower the surface free energy penalty the system has to pay upon generating oil-water interface associated with the liquid protrusion. The key role of surfactants in this reaction scheme was experimentally verified by studying dumbbell-formation in the absence of amphiphiles. These procedures yielded ill-defined particles without any well-defined protrusions (see Supporting Information S3).

Since the formed liquid protrusions consists of monomer, they are easily solidified by addition of an oil-soluble polymerization initiator (Scheme 2, step d) to yield the desired dumbbell-shaped particles.

Evidently, the large number of experimental variables associated with the four reaction steps depicted in Scheme 2 opens opportunities to extensively tune the geometry of the resulting chemically anisotropic dumbbell-shaped colloids. We choose to investigate the effect of the properties of the outer (chlorinated) layer, the cross-link density in both seed and protrusion and the volume of monomer used to swell the chlorinated seeds (swelling ratio). Based on literature regarding emulsion-based procedures to synthesize anisotropic colloids, we expect that these variables have the most significant influence on the final particle geometry [1–13].

We must note that besides the formation of the desired dumbbell-shaped particles also a small fraction (typically 5–10%, as determined with TEM) of larger clusters is formed [1]. These clusters form when (partially) liquid protrusions of multiple monomeric dumbbells fuse before or just after polymerization is initiated. Most abundant are clusters formed after merging of two dumbbells, which will be referred to as two-patch particles since they carry two chlorinated regions (Scheme 3). The fraction of formed dimers is set by the chance two individual dumbbells meet. Naturally, this chance depends on the size of the liquid protrusion and on the time between forming the liquid protrusions and actual polymerization of these monomer droplets. Additionally, the con-

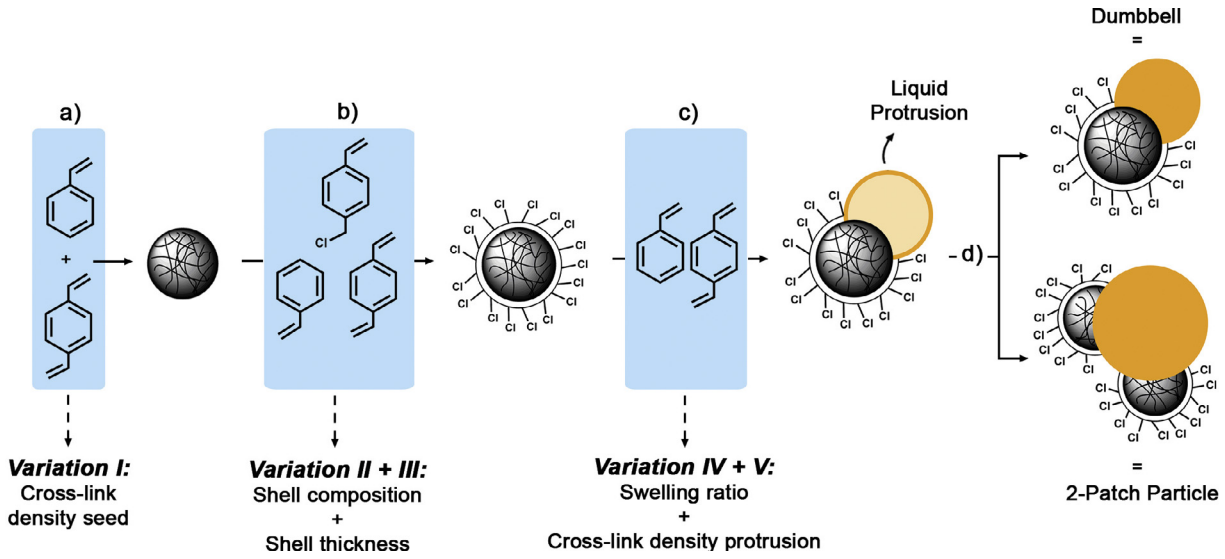

Scheme 2. Schematic representation of the synthesis of chemically anisotropic dumbbell-shaped colloids that consist of a non-functionalized patch (yellow) and a functional, chlorinated lobe. Step (a): emulsion polymerization of styrene and divinylbenzene (DVB) to prepare cross-linked polystyrene seeds. Step (b): seeded-emulsion polymerization of mixtures containing 4-vinylbenzyl chloride (VBC), DVB and styrene in the presence of cross-linked polystyrene particles. Step (c): swelling of the chlorinated seeds with a DVB/styrene mixture and subsequent formation of a liquid protrusion by heating the monomer-swollen seeds. Step (d): polymerization of the liquid protrusion to yield solid, chemically anisotropic dumbbells (top, right). If liquid protrusions of two individual dumbbells merge before or just after polymerization is induced, two-patch particles are formed (bottom, right). The variations applied throughout this article are listed at the bottom of the scheme.

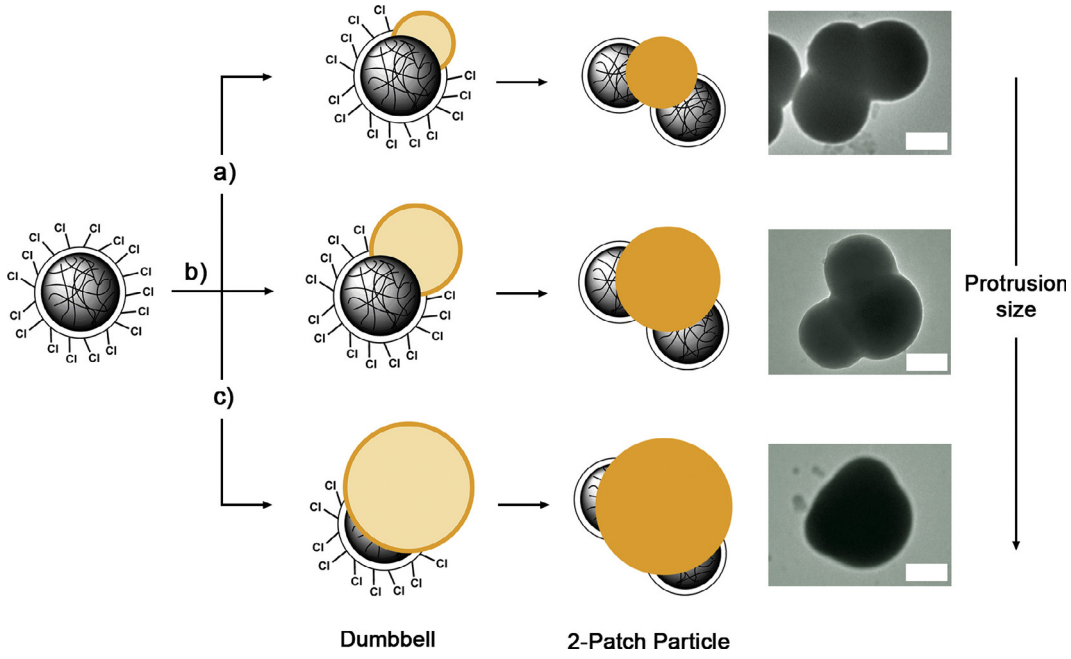

Scheme 3. Schematic representation of chlorinated particles with liquid protrusions on their surface and the two-patch particles they form after merging of the liquid protrusions of two individual dumbbells. The yellow central domain of the two-patch particles originates from the fused protrusions. With increasing protrusion size, the geometry of resulting two-patch particles becomes more spherical. On the right side of the scheme, transmission electron microscopy (TEM) images of typical two-patch particles are depicted. Scale bars for the top two figures = 0.2 μm and for the image in the bottom right corner 0.5 μm.

centration of surfactants in the reaction mixture has an influence on the fusion propensity of the liquid protrusions. If the monomer droplets are stabilized to a lesser extent, fusion is more likely. In all procedures described in this article, polymerization was induced directly after protrusion formation and surfactant concentrations well above the critical micelle concentration (CMC) were employed to minimize the formation of higher order patchy particles. Although a side-product if dumbbell-shaped colloids are aimed for, the presence of these two-patch particles can be used to our advantage. Since these two-patch particles are formed by fusion of protrusions of two individual dumbbells, the volume of this central domain is equal to two times the volume of a single protrusion. Therefore, the geometry of the two-patch particles can be used to deduce which lobe of monomeric dumbbells corresponds to the chlorinated seed and which one to the newly formed protrusion. This procedure is schematically depicted in Scheme 3. Protrusions smaller than the seed will result in more linear two-patch particles, while fusion of dumbbells with larger protrusions gives rise to

more spherical dimers with a significantly larger central lobe. Because of this convenient method to distinguish between seed lobe and newly formed protrusions, no attempts were conducted to separate dumbbells from the higher-order patchy particles. If, however, dispersions with solely dumbbells or multiple-patch particles are required, these colloids can be separated via density gradient centrifugation [1].

In the upcoming sections systematic variations of the aforementioned experimental parameters will be carried out to probe their effect on the particle geometry.

3.2. Effect of the swelling ratio

The most straightforward strategy to alter the size ratio, *i.e.*, the diameter of the seed divided by the diameter of the protrusion, is by varying the swelling ratio. The swelling ratio used throughout this paper is defined as the mass of added monomer divided by the total mass of polymer present in the seed dispersion (Scheme 2, step c, variation **IV**). In principle, the size of the resulting protrusion is directly related to the swelling ratio. Theoretically, the lower limit of the protrusion size is determined by the minimal amount of monomer required to swell the seed to such an extent that enough elastic force can be generated to facilitate monomer phase separation [14,15]. The upper limit is obviously set by the amount of monomer the seeds can accommodate during the swelling step. Since polystyrene colloids can be swollen with volumes of styrene up to several times their own volume, protrusions with dimensions exceeding those of the employed seeds should be within reach [1–3,14,15].

We prepared dumbbell-shaped colloids starting from a single batch of chlorinated seeds with five different swelling ratios (0.5, 1, 4, 6 and 10, Table S1, entry 3–7). The particles were swollen with pure styrene, resulting in protrusions consisting of non-cross-linked, linear polystyrene. Representative transmission electron microscopy (TEM) images of the resulting colloidal dumbbells are shown in Fig. 1. Evidently, the low swelling ratio of 0.5 did not result in formation of anisotropic colloids (Fig. 1a). Despite the fact that the particles are slightly larger after polymerization and therefore were able to take up the added monomer, the low degree of swelling clearly fails to induce enough elastic stress onto the seed's polymer network to actually drive the monomer phase separation.

By increasing the swelling ratio to 1 or 4, asymmetric dumbbells could be prepared with protrusions smaller than the chlorinated seed as deduced from the approximately linear geometry of present two-patch particles (see Scheme 3). Evidently, the protrusions produced employing a swelling ratio of 1 (Fig. 1b) are significantly smaller than those obtained for swelling ratio 4 (Fig. 1c).

Going up to swelling ratios of 6 and 10 yielded slightly larger protrusions resulting in shape-symmetric dumbbells (Fig. 1d and e). No significant geometric change was observed by going from swelling ratio 6 to 10. After protrusion formation, the lobes corresponding to the chlorinated seeds were of comparable size regardless of the swelling ratio. This strongly implies that these symmetric dumbbells carry the maximum achievable protrusion size since simply not all monomer was absorbed by the seed particles in the swelling stage. In agreement with this statement is the observation that the formed protrusions are significantly smaller than one would expect based on the swelling ratio alone. As mentioned before, conventional polystyrene particles are able to take up monomer volumes several times larger than their own volume, so clearly the limited swelling capacity is a consequence of the core-shell layout of our chlorinated seeds. Directly coupled to this restricted monomer uptake is the inability to grow protrusions larger than the employed seed particles. In Section 3.5.1 this limitation will be systematically investigated in further detail.

3.3. Cross-linking of the protrusion

In the previous section, dumbbell-shaped colloids with non-cross-linked protrusions were prepared. As long as these anisotropic colloids remain dispersed in media incapable of dissolving polystyrene, the absence of cross-linking will not affect the particle geometry and morphology. However, if the particles are dispersed in a good solvent for polystyrene, *e.g.*, dimethylformamide (DMF) or tetrahydrofuran (THF), the protrusion's linear polymers will dissolve leading to complete disappearance of the protrusion (Fig. 2a and b). This limited solvent compatibility restricts the applicable reaction conditions to convert the surface chlorine groups to desired (end-) functionalities and therefore to fully exploit the chemical versatility of the surface benzyl chloride moieties.

To overcome the limited range of solvents applicable for chemical transformations of the benzyl chlorides, the protrusions should also be cross-linked. As for the seeds, linking individual polymers to form a (single) network prevents dissolution. The most natural approach to prepare cross-linked protrusions is by swelling the seeds with a mixture of styrene and cross-linker (divinylbenzene, DVB). We can safely assume that the liquid protrusion formed after phase separation will contain styrene and DVB in a comparable ratio as present in the monomer mixture used to swell the chlorinated seeds. The presence of DVB ensures that subsequent polymerization will directly result in cross-linked protrusions.

To investigate the effect of the DVB concentration in the swelling solution on the resulting particle geometry (Scheme 2, variation **V**), chlorinated seeds were swollen with styrene containing 0, 3, 6, 12 and 20 vol% DVB (Table S1, entry 2, and 8–11). In all cases, the total swelling ratio was kept constant at a value equal to 6. Typical TEM images of the obtained colloids are shown in Fig. 3. Although for all degrees of cross-linking well-defined dumbbells were obtained, the contact angle becomes less pronounced at intermediate cross-link densities (3 and 6 vol%, Fig. 3b and c) compared to the particles with protrusions that are not cross-linked (Fig. 3a). Apparently, the degree of phase separation between seed and protrusion decreases with increasing cross-link density. Increasing the cross-link density even further to 12 vol% resulted in a smaller protrusion despite a constant swelling ratio for all dumbbell-formation reactions within this experimental series (Fig. 3d). The size of the protrusions reduces even further at the highest DVB content of 20 vol% (Fig. 3e). At these extremely high cross-link densities, a significant fraction of seed particles did not even produce a protrusion as highlighted by the white arrows in Fig. 3e.

These observations can be rationalized if we consider the formation mechanism of the protrusions proposed by Sheu et al. (Scheme 1, step d and e) [14,15]. According to their nucleation and growth type of mechanism that causes protrusion formation, only a small initial liquid protrusion is formed after elastic contraction of the seed's polymer network. The remaining monomer remains inside the swollen seed particle. During polymerization of the liquid lobe, monomer is consumed and an osmotic flow of monomer is generated from the swollen seed to the protrusion. Naturally, this flow is obstructed by the forming polymer (network) which induces an increased local viscosity. This viscosity is strongly influenced by the degree of chemical cross-links in the forming polymer network and hence directly related to DVB concentration in the swelling solution. Swelling with mixtures containing higher concentrations of DVB therefore counteracts monomer phase separation, leading to dumbbell-shaped particles with less separated or even smaller protrusions.

Tuning the concentration of cross-linker in the swelling solution therefore provides means to control the aspect-ratio of the particles as well as the size of the protrusions. Furthermore, the

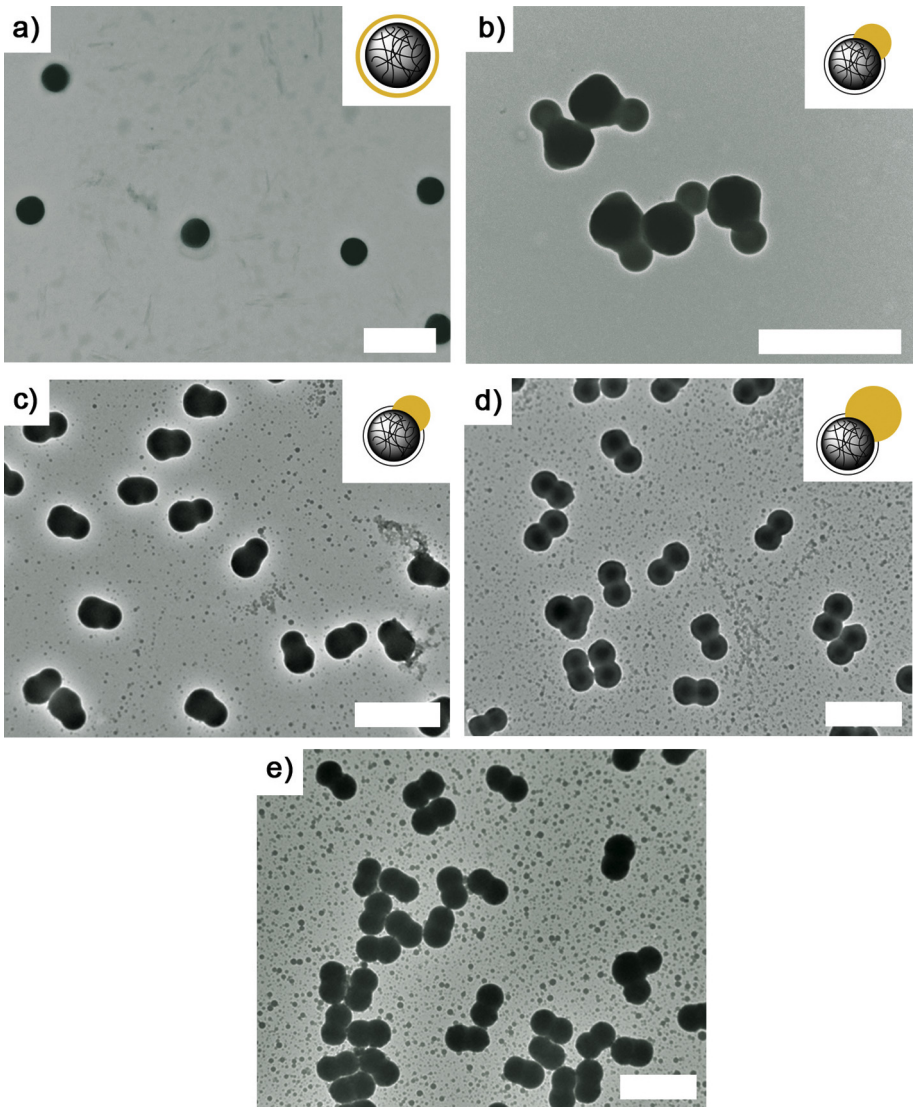

Fig. 1. Transmission electron microscopy (TEM) images of dumbbell-shaped colloids prepared employing swelling ratios of (a) 0.5, (b) 1, (c) 4, (d) 6 and (e) 10 using chlorinated core-shell colloids as seed particles. In all cases the protrusions were not cross-linked. Scale bar = 1 μm for all panels.

use of cross-linker as part of the swelling mixture yields colloids that are chemically resistant against solvents capable of dissolving linear polystyrene (Fig. 2c and d).

3.4. Effect of the cross-link density of the seed particles

As discussed in the Introduction, expulsion of liquid monomer from a monomer-swollen seed is induced by an elastic contraction of the cross-linked polymer network inside the seed particle. To form a liquid protrusion, the generated elastic-retractile force must exceed the sum of the mixing and interfacial forces [14,15]. Since the contraction force that can be generated depends on the stiffness, and therefore on the cross-link density of the polymer network we expect there is a minimal cross-link density required to drive the monomer phase separation. Below this critical cross-link density, no phase separation occurs, and the monomer remains trapped in the interior of the seeds.

Following this reasoning one may conclude that using seed particles with a higher cross-link densities results in a more pronounced phase separation and hence in a large degree of shape anisotropy. However, we have to consider that increasing the cross-link density is inextricably coupled to a reduction of the network flexibility. The decreased flexibility of these networks translates into a lower swelling capacity compared to their loosely cross-linked counterparts. Although these particles might be capable of generating larger elastic-retractile forces, a smaller monomer volume is available to expel. Naturally, this translates into particles with smaller protrusions.

Based on this reasoning we expect an optimum in the protrusion size when varying the cross-link density of the seeds. To test this hypothesis we prepared seed particles with cross-link densities ranging from 1 to 18% (Table S1, entry 8, 12–22). The cross-link density was easily varied by changing the ratio between monomer and cross-linker in the (seeded) emulsion polymerization steps (Scheme 2, step a and b, variation **I**). The chlorinated shells were cross-linked with the same density as that of the employed polystyrene core particles in order to keep the cross-link density as uniform as possible throughout the whole seed particle. Variations of the concentration of cross-linker had minor effect on both particle size/polydispersity (Table S1, entry 8, 12–22) and chlorine content as probed with dynamic light scattering (DLS) and infrared (IR) spectroscopy, respectively.

For each degree of cross-linking, dumbbell-formation was attempted with swelling ratios of 6 and 10. The (anisotropic)

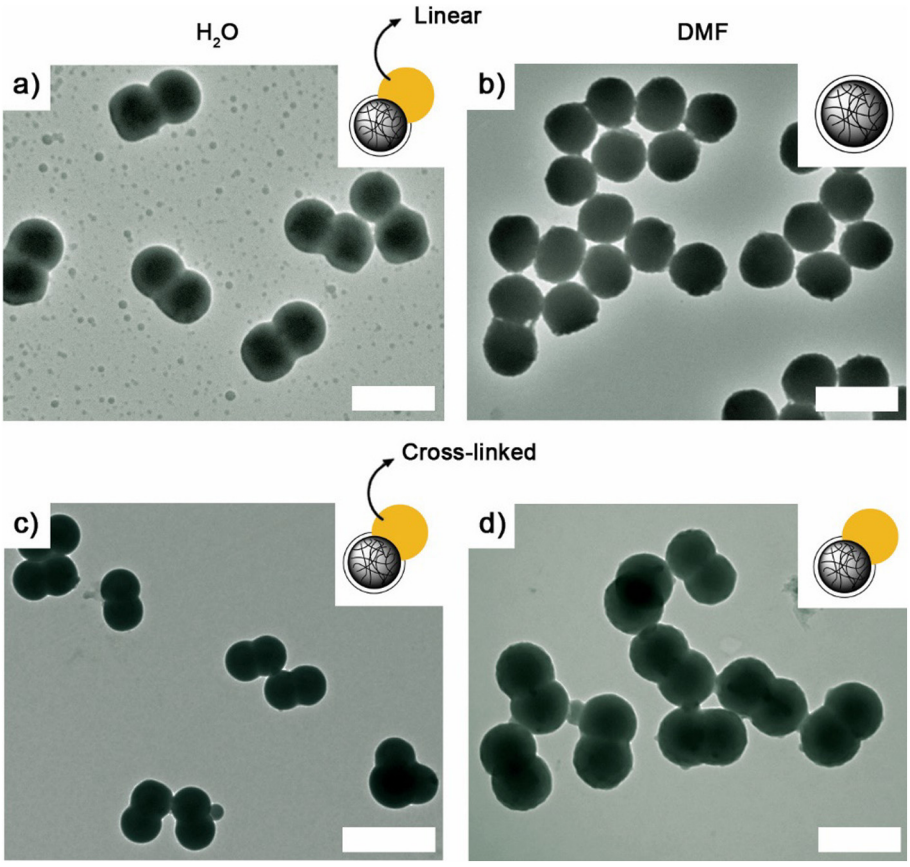

Fig. 2. Transmission electron microscopy (TEM) images of dumbbell-shaped colloids with (a) non-cross-linked (linear) protrusions and (c) cross-linked protrusions. Introducing the dumbbells in dimethylformamide (DMF) at room temperature results in instantaneous dissolution of the linear protrusion (b), while the dumbbells with cross-linked protrusions remain intact (d). Scale bar = 0.5 μm for all panels.

particles obtained employing a swelling ratio of 10 are depicted in Fig. 4. The results obtained by using swelling ratio 6 can be found in Supporting Information S4 and follow the same general trends as the results presented here.

Employing chlorinated seeds with a cross-link density of only 1% in the protrusion formation procedure (Table S1, entry 12 and 13) yielded relatively spherical particles without well-separated protrusions (Fig. 4a). In agreement with the previously mentioned hypothesis, these loosely cross-linked polymer networks are too flexible to provide enough elastic stress to induce significant monomer phase-separation. TEM analysis of the product dispersion revealed the presence of a small fraction of larger aggregates (≈5%). These clusters most probably form when the swollen, and therefore soft, colloidal particles bump into each other and get stuck during the final polymerization process.

Upon increasing the cross-link density of the seed particles to 2 or 3% (Table S1, entry 8, 14–16) the anisotropy of the particles clearly increases (Fig. 4b and c). The more pronounced degree of phase separation is in agreement with the expectation that more densely cross-linked networks generate a stronger driving force for monomer phase separation. The small increase in the cross-link density from 1 to 2–3% illustrates that the resulting particle geometry is highly sensitive towards this experimental variable.

A further increase in the cross-link density did not result in the formation of larger protrusions or particles with more pronounced anisotropy. Employing seed particles with a cross-link density of 5% showed the formation of asymmetric particles in which the protrusion is smaller than the corresponding seed particle for both swelling ratios (Table S1, entry 17 and 18, Fig. 4d). The observed decrease in protrusion size was anticipated based on decreased swelling capacity of seeds with increasing cross-link density.

Raising the cross-link density even further to 10 and 18% (Table S1, entry 19–22) resulted in the formation of 'popcorn-like' particles (Fig. 4e and f). Polymer networks with these high cross-link densities are known to be inhomogeneous [14,15]. If phase separation between monomer and these networks occur, the contraction of the network will be localized within the regions containing the weakest spots, leading to the formation of multiple, ill-defined protrusions. An additional contribution to the formation of multiple protrusions might be an increased surface roughness of the chlorinated seeds at higher cross-link densities [3]. Enhanced surface roughness with increasing cross-link density is commonly observed for several types of polymer colloids, including chlorinated core-shell particles [33,34]. It is reasonable to assume that during the very early stages of monomer separation from the swollen seeds yields multiple small liquid lobes. If these lobes are mobile over the particle surface, they will merge to minimize the total oil-water interface and form one large protrusion. However, if the surface is rough, the small individual liquid lobes might get pinned on the surface, making fusion to just one protrusion not possible. Polymerization of these individual monomer protrusions will eventually yield the observed 'popcorn-like' particles.

Based on the experimental results obtained after varying the cross-link density of the seed particles we can conclude that chlorinated seeds with a cross-link density between 2 and 3% provide dumbbell-shaped colloids with the most pronounced anisotropy. These degrees of cross-linking providing an ideal compromise

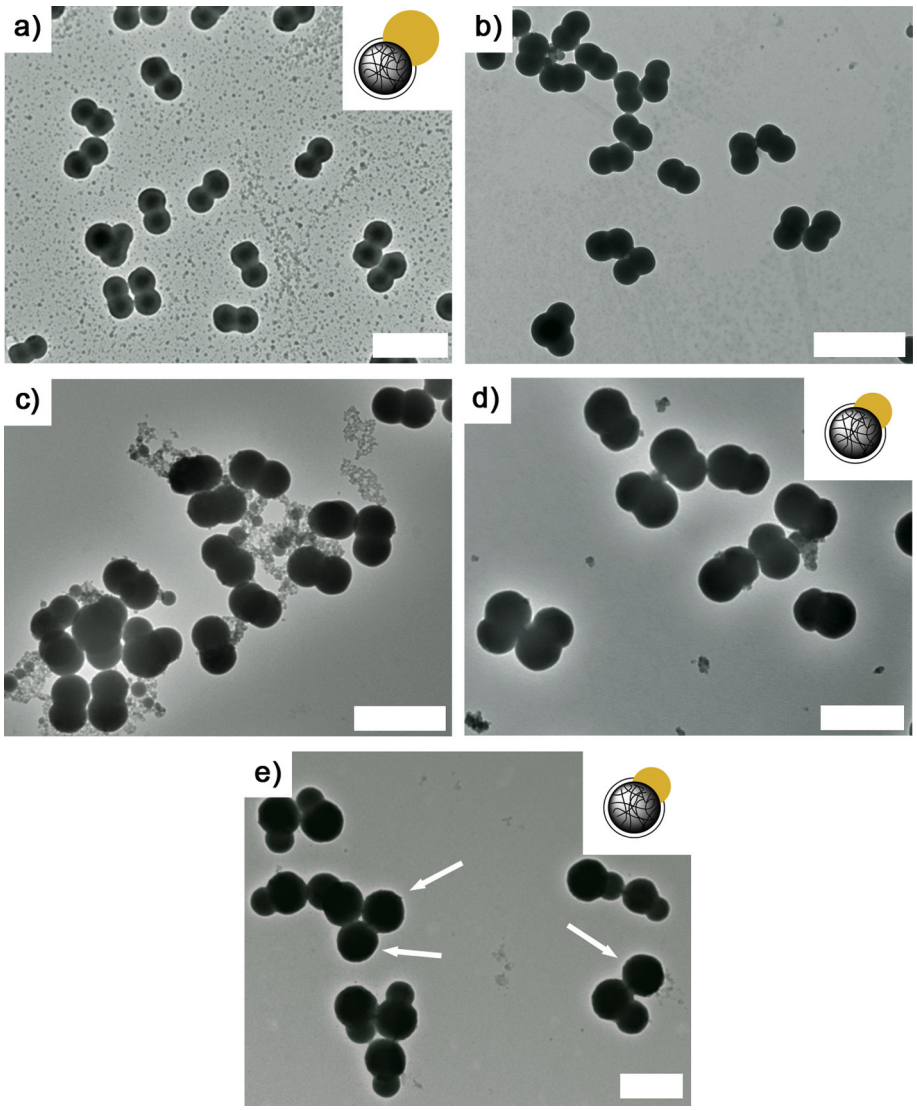

Fig. 3. Transmission electron microscopy (TEM) images of anisotropic particles obtained after swelling chlorinated seed particles with styrene containing (a) 0, (b) 3, (c) 6, (d) 12 and (e) 20 vol% divinylbenzene (DVB) to form a (cross-linked) protrusions. Scale bar = 1 μm for panels a, b and c. Scale bar = 0.5 μm for panel d and e.

between swelling capability and ability to generate enough force to drive the monomer phase separation.

3.5. Effect of the shell properties on dumbbell formation

As depicted in Scheme 2 and outlined in the Introduction, a key step in the formation process of the (chemically) anisotropic colloids is the introduction of a chlorinated layer on the seed particles. The properties of this shell are expected to significantly influence the geometry of the resulting dumbbell-shaped colloids by determining the contact angle of the expelled liquid monomer.

Inspired by the experiments performed by Mock et al., we systematically vary both shell composition and thickness to probe how these parameters influence the final particle geometry [20]. Furthermore, systematic variation of the shell properties might elucidate why the accessible particle geometries described in the previous sections are limited to symmetrical dumbbells and colloids with protrusions smaller than the chlorinated seed only. Overcoming this limitation in accessible particle shapes by, for example, preparing particles with protrusions larger than the chlorinated seeds is a key step in fully exploiting the potential of these building blocks in future (self-assembly) studies.

3.5.1. Shell thickness

The primary role of the shell on our particles is to increase the hydrophilicity of the surface. Enhanced hydrophilicity aids in preventing full wetting of the expelled monomer and therefore enables formation of well-defined (liquid) protrusions. Furthermore, the presence of a hydrophilic particle surface facilitates swelling of the seeds by lowering the surface tension between the seed and the aqueous continuous phase (last term in Eq. (1)). To fulfill these functions only a very thin surface layer of p(VBC) should suffice. Moreover, we expect that thick hydrophilic shells might even hamper efficient dumbbell formation, since swelling of the seed particle by hydrophobic monomer becomes more difficult if a larger fraction of the particles is (slightly) hydrophilic (see Section 3.1). Thin shells should therefore promote swelling and thereby enabling preparation of dumbbell-shaped colloids with larger protrusions.

To verify this hypothesis, seeds particles with a variety of chlorinated shell thicknesses were prepared. Control over the shell thickness was easily achieved by simply varying the volume of VBC added to a fixed number of polystyrene particles in the seeded emulsion polymerization step (Scheme 2, step b, variation **III**). In all cases, the added VBC contained 3 vol% DVB to match the

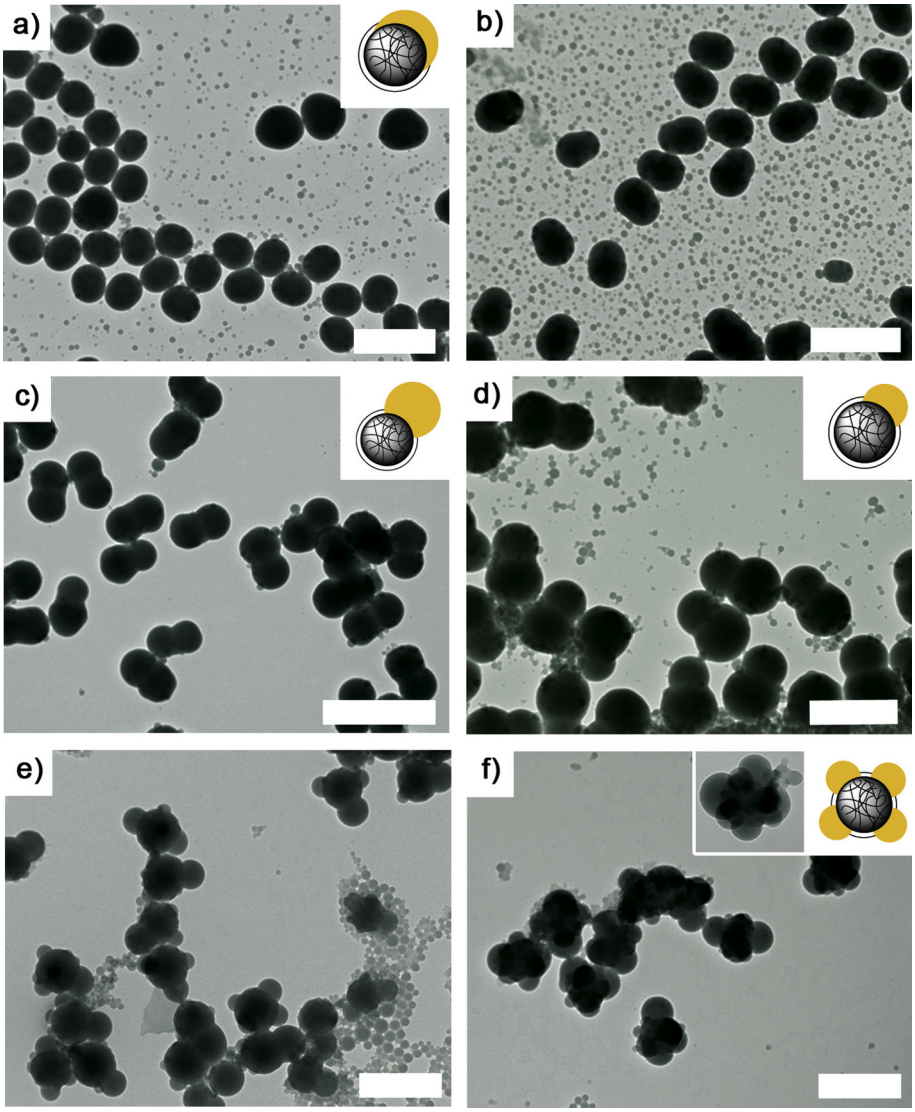

Fig. 4. Transmission electron microscopy (TEM) images of anisotropic particles prepared using seed particles with cross-link densities of (a) 1%, (b) 2%, (c) 3%, (d) 5%, (e) 10% and (f) 18%. All reactions were performed with a swelling ratio of 10. Scale bar = 0.5 μm for all panels.

cross-link density of the employed seed particles. Using this strategy, chlorinated layers consisting of cross-linked p(VBC), ranging from 8 to 65 nm were introduced on the same batch of seed particles (Table S2, entry 1, 3–10). The thicknesses of the chlorinated layers were estimated from DLS data by measuring the increase in hydrodynamic radius compared to the seed particles (Fig. 5a, black squares). All syntheses yielded monodisperse particles, as reflected by the low polydispersity indices (PDIs, Fig. 5a, red triangles). Furthermore, IR spectroscopy showed a clear increase in chlorine content ($-CH_2-Cl$ vibration at 1266 cm^{-1}) with increasing shell thickness (Fig. 5b, highlighted in grey) [29].

For each of the chlorinated core-shell seeds, two dumbbell syntheses were performed with swelling ratios 6 and 10. The (anisotropic) particles obtained employing a swelling ratio of 10 are depicted in Fig. 6. The results obtained by using swelling ratio 6 can be found in Supporting Information S5 and are comparable to the results presented here.

We found that the thickness of the cross-linked chlorinated shell has a distinct influence on the size of the protrusions that are formed. The particles with the thinnest shell (8 nm, Table S2, entry 9 and 10), did not yield dumbbell-shaped, but spherical colloids (Fig. 6a). Increasing the shell thickness to 27 nm (Table S2, entry 7 and 8) led to the formation of asymmetric dumbbell-shaped particles with a slightly better defined contact angle (Fig. 6b). The formed protrusion was smaller than the seed particle, as deduced from the shape of two-patch particles present in the product dispersion (Scheme 3). Chlorinated particles with 33 nm thick shells (Table S1, entry 6 and 16) resulted in the formation of well-defined symmetric dumbbells (Fig. 6c). Similar particle geometries were obtained using seed particles with 45 nm chlorinated shells (Table S2, entry 5 and 6, Fig. 6d). Increasing the thickness of the chlorinated shell even further resulted in the formation of ill-defined seed particles. Although capable of protrusion formation, the surface texture on these seeds, as observed with TEM, makes these colloids not ideal candidates for studying the effect of shell thickness on the protrusion formation process. For these ill-defined seeds, predominantly asymmetric dumbbells were formed with protrusions smaller than the seeds (Table S2, entry 3 and 4).

Excluding the ill-defined chlorinated seeds with the thickest chlorinated shells, the protrusion size increases with increasing thickness of the chlorinated layer. Contradictory to our expectation that the swelling capacity of the chlorinated seeds is predominantly determined by the volume of the highly hydrophobic

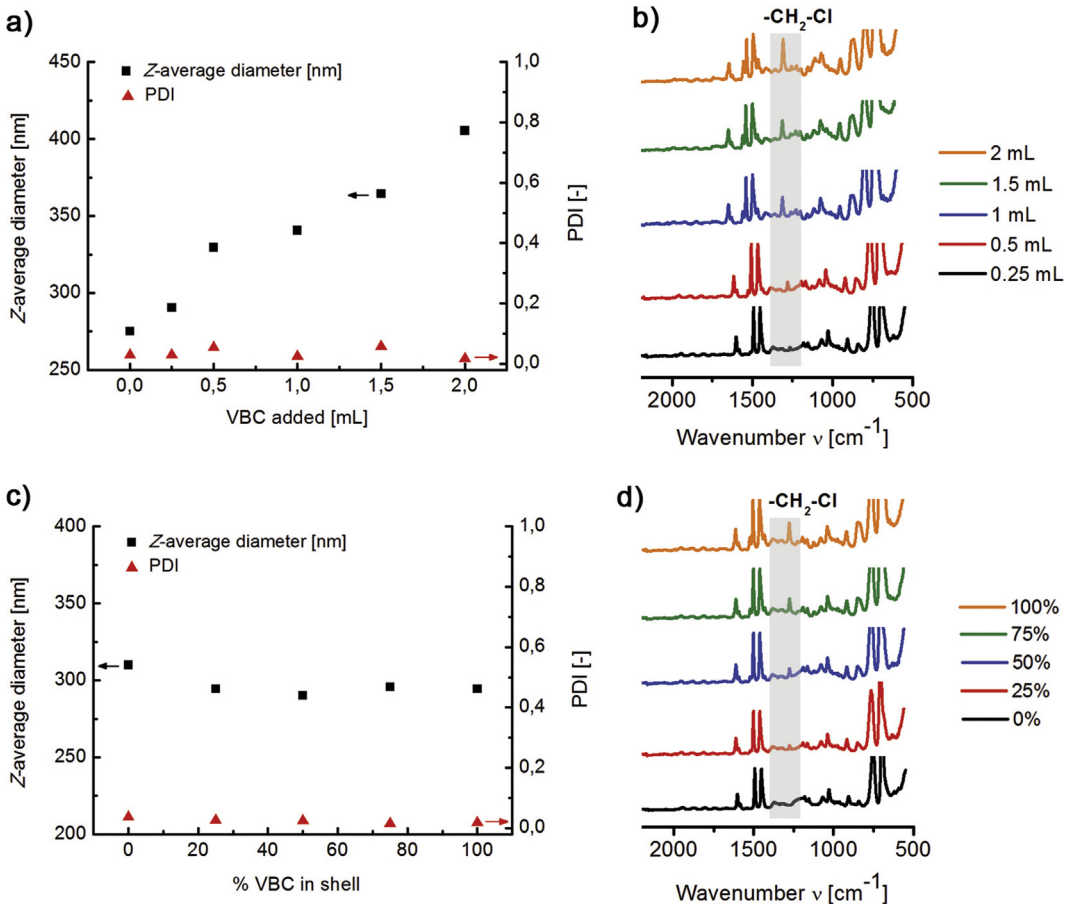

Fig. 5. (a) Dynamic light scattering (DLS) results of the core-shell seed particles prepared by addition of a variable amount of 4-vinylbenzyl chloride (VBC) to a fixed number of cross-linked polystyrene particles. The VBC added to the core particles contained 3 vol% divinylbenzene (DVB) in each synthesis. The *Z*-average sizes are shown in black squares and polydispersity indices (PDIs) are represented by the red triangles. (b) Infrared (IR) spectra obtained for the core-shell seed particles upon varying the chlorinated shell thickness. The highlighted signal at 1266 cm^{-1} corresponds to the $-CH_2-Cl$ vibration. (c) DLS results of the core-shell seed particles prepared by the addition of a mixture of styrene and VBC to a fixed number of core particles. The volume percentage of VBC in the feed ranged from 0% to 100%. All monomer mixtures contained 3 vol% DVB. The *Z*-average sizes are shown in black squares and polydispersity indices (PDIs) are represented by the red triangles. (d) IR spectra obtained for the core-shell seed particles with upon varying the shell composition. The signal at 1266 cm^{-1} corresponds again to the $-CH_2-Cl$ vibration.

polystyrene core, these results suggest that only the outer shell is actively involved in the swelling and subsequent protrusion formation process. This suggestion is supported by the observation that the particles with thin chlorinated shells did not grew significantly after attempted protrusion formation. The low uptake of monomer in the swelling step does not induce sufficient stress on the polymer network of the seeds, explaining the absence of protrusions on these particles, even though the outer surface of the particles was coated by p(VBC) (Fig. 5a and b). By increasing the shell thickness, more monomer can be adsorbed leading to a stronger driving force for phase separation and hence larger protrusions.

Clearly, the TEM images shown in Fig. 6 contradict our previous stated hypothesis that a thinner shell should promote swelling capacity of the particles. A possible explanation for the low swelling capacity of the seeds can be provided if the internal structure of the employed core-shell seed particles is examined in more detail. Nieuwenhuis et al. [35] showed by means of scattering techniques that the cross-link density in a latex particle is non-uniform. The crosslink density decreases with the radial distance from the particle center. McPhee et al. [36] confirmed this picture by measuring the efficiency of cross-linking monomer incorporation into growing particles during an emulsion polymerization. They concluded that a large portion of the cross-links were incorporated during the initial growth of the particles. This is not surprising, as the solubility of a polymer chain decreases with increasing molecular weight; addition of cross-linking monomer facilitates a substantial increase in polymer length and therefore its insolubility. These insoluble, highly cross-linked macromolecules crash out of solution and act as nuclei for the formation of the final latex particles.

If we extrapolate the findings of Nieuwenhuis et al. and McPhee et al., we obtain the following picture for the detailed internal structure of the employed chlorinated core-shell particles: the grey area in Fig. 7a represents the polystyrene core (CPs) while the chlorinated shell is depicted by the white outer layer. Both layers are cross-linked as indicated by the presence of the black wavy lines. Since the particles are prepared in a two-step process, a densely cross-linked region will be formed in the early stages of each emulsion polymerization (yellow highlighted areas in Fig. 7a). The initial polymerization (Scheme 2, step a) yields particles with a highly cross-linked core. Growing a shell around these particles via a seeded-emulsion polymerization (Scheme 2, step b) generates a more densely cross-linked interfacial layer between the grey polystyrene core and the chlorinated outer layer (Fig. 7a).

The presence of this inhomogeneous distribution of cross-link density within a chlorinated core-shell particle is experimentally verified by etching the particles with organic solvents, *e.g.*, dimethylformamide (DMF) or tetrahydrofuran (THF). Before etching, the particles are homogeneous in appearance as observed with TEM (Fig. 7b). However, upon chemical treatment with DMF or

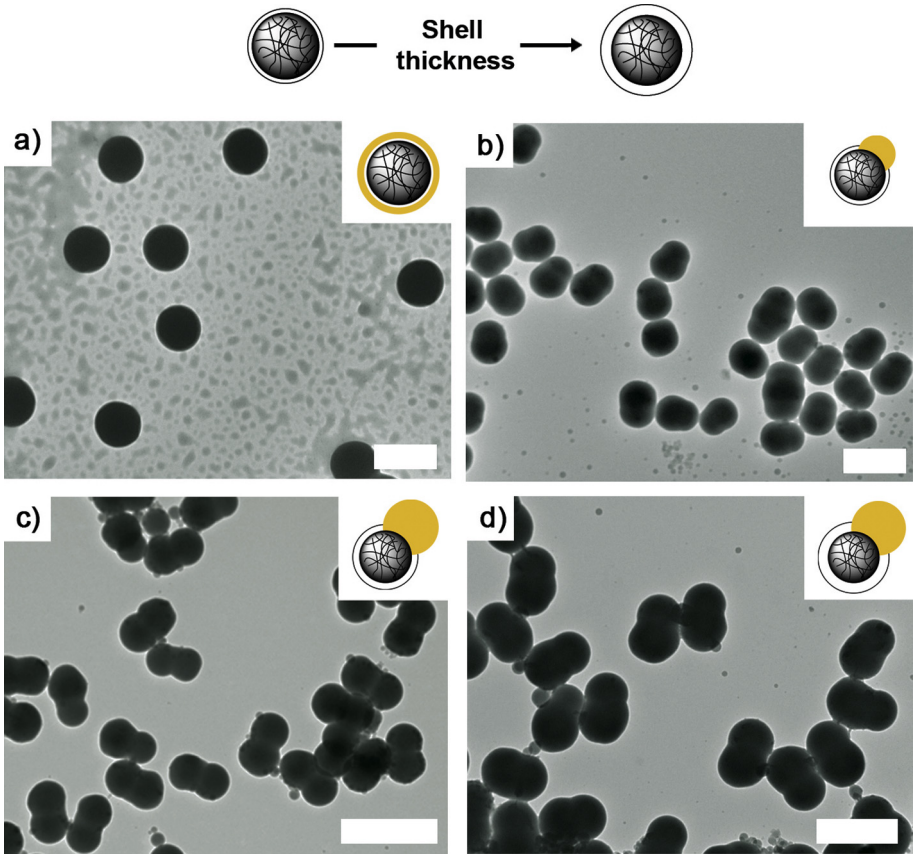

Fig. 6. Transmission electron microscopy (TEM) images of dumbbell-shaped colloids prepared by using core-shell seed particles with chlorinated shell thicknesses of (a) 8 nm, (b) 27 nm, (c) 33 nm and (d) 45 nm in combination with a swelling a ratio of 10. Scale bar = 0.5 μm for all panels.

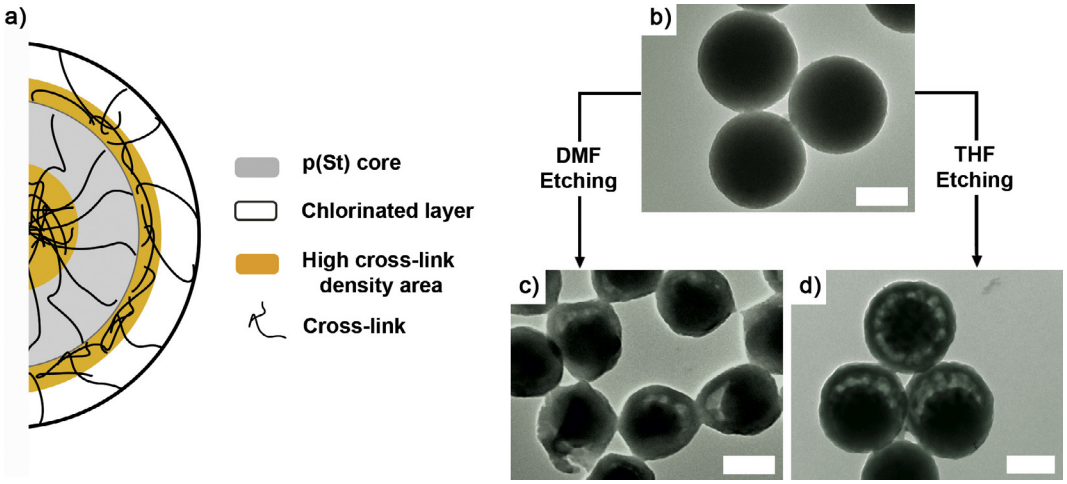

Fig. 7. (a) Schematic representation of variations in cross-link density in the interior of a single chlorinated core-shell colloid. Cross-links are depicted by the black lines. The grey area represents the polystyrene core (CPs) and the white outer ring the chlorinated layer. Higher cross-link density areas are highlighted in yellow and are located in the center of the particle and on the interface between the core and the outer chlorinated layer. (b) Transmission electron microscopy (TEM) image of chlorinated particles before etching. (c) TEM images of chlorinated particles after etching with (c) dimethylformamide (DMF) for 24 h at 90 °C and (d) tetrahydrofuran (THF) for 24 h at 25 °C. Scale bar = 0.2 μm for all panels.

THF, the particles reveal a yolk-shell structure (Fig. 7c and d). The loosely cross-linked (or even linear) part of the colloid dissolved, leaving behind the densely cross-linked core and interfacial layer. Furthermore, the size of the particles decreased after the etching procedure, indicating that the surface layer of the chlorinated coating was also dissolved and therefore only marginally cross-linked. Additional TEM images of the etched colloids can be found in Supporting Information S6.

Naively, one might argue that when these core-shell particles are swollen with hydrophobic monomers the highly cross-linked interfacial region between the seed and shell acts as a barrier for the monomer to penetrate into the core. Due to a locally increased

viscosity caused by a high concentration of chain entanglement monomer does not diffuse freely into the bulk of the chlorinated particles. In effect, the actual swelling capacity of the seed particle as a whole is only determined by the volume of the outer shell. This reasoning explains the observation that protrusion sizes increase with increasing shell thickness. By increasing the available network volume for swelling, more monomer can be accommodated inside these particles resulting in formation of larger protrusions. Nevertheless, the presence of the highly cross-linked interfacial region restricts the swelling capacity of the seeds and therefore the maximum achievable protrusion size (see Section 3.1).

The presence of the highly cross-linked interfacial region could in principle be prevented by growing a non-cross-linked layer onto the polystyrene particles (Table S2, entry 17). However, upon swelling these particles with a large volume of styrene, the shell most likely dissolves. Dissolution results in a loss of surface hydrophilicity of the seeds. Protrusion formation is therefore no longer possible, since expelled monomer will simply wet the hydrophobic outer surface of the non-soluble cross-linked polystyrene core. Previously reported seed particle which relied on covalently bound, but non-cross-linked layers of poly(acrylic acid) or poly(vinyl acetate) do not suffer from this dissolution process, since these polymers are significantly more hydrophilic than our chlorinated coatings and therefore not soluble in the added hydrophobic swelling monomer [1,20]. Experimental evidence for the lack of protrusion formation ability and loss of chlorine moieties after attempted protrusion formation of seeds with non-cross-linked chlorinated layers is summarized in Supporting Information S7.

A second possibility to circumvent the presence of a densely cross-linked layer between the seed and the chlorinated shell is to prepare particles which consist of only one polymer network and a gradient in the VBC content. These particles are in principle accessible by conducting a one-pot emulsion polymerization in which VBC is added to the reaction mixture at moderate to high styrene conversions. A disadvantage of this procedure is the decreased number of surface chlorines compared to the well-defined core-shell particles used throughout this study. The decreased chlorine surface density might results in seeds that are not hydrophilic enough for efficient protrusion formation. Nevertheless, this route is potentially interesting and is recommended for future follow-up research.

3.5.2. Effect of shell composition

With the strong experimental suggestion that only the shell participates in swelling and subsequent dumbbell formation (see Section 3.5.1), we attempted to increase the swelling ability of these outer layers by using mixtures of styrene and VBC as shell monomers (Scheme 2, step b, variation **II**). Using styrene as co-monomer results in more hydrophobic shells which should be able to accommodate more monomer in the swelling step. Since VBC is slightly more hydrophilic than styrene we expect that the majority of this monomer will be located at the particle surface to provide both the chemical handle and the required slightly enhanced surface hydrophilicity.

Based on a single batch of cross-linked polystyrene particles, five different seed particles were prepared with shells consisting of 0, 25, 50, 75 and 100 vol% VBC (Table S1, entry 16, Table S2, entry 1, 2, 11–16). Throughout these syntheses, the total monomer volume added to the polystyrene cores was kept constant and the shell was cross-linked by adding 3 vol% DVB to the monomer phase. DLS measurements revealed we obtained core-shell particles with a shell thickness of approximately 30 nm. This thickness was found to be independent of the shell composition (Fig. 5c). IR spectroscopy confirmed an increasing chlorine content if higher ratios of VBC:St were used to grow the shell (Fig. 5d). In other words, the composition of the monomer feed is directly transferred to the composition of the shell. Furthermore, all seeded emulsion polymerizations yielded monodisperse particles (low PDIs, Fig. 5c, red triangles), making the synthesized colloids an ideal series to test the influence of the shell composition.

Subsequently, each type of (chlorinated) seed was used to prepared dumbbell-shaped colloids using swelling ratios equal to 6 and 10. Representative TEM images of the obtained particles after employing a swelling ratio of 10 are shown in Fig. 8. The results obtained by using swelling ratio 6 can be found in Supporting Information S8.

In agreement with previously reported results, the absence of a hydrophilic coating prevents formation of well-defined protrusions (Table S2, entry 2, Fig. 8a). Shells that were grown by the addition of solely styrene are simply too hydrophobic to prevent the expelled monomer from fully wetting the seed surface. Despite the presence of charged sulfate and sulfonates moieties originating from the initiator system (KPS and $NaHSO_3$), which generate a strongly negative zeta (ζ) potential of -50 mV, the surface hydrophilicity proved to be insufficient [37].

Similarly, employing particles which contained only 25 (Table S2, entry 15 and 16) or 50 vol% (Table S2, entry 13 and 14) of VBC in their shell did not result in well-defined dumbbell-shaped colloids either (Fig. 8b and c). Especially the particles with the lowest chlorine content resulted in spherical particles regardless of the swelling ratio. One could also claim that the seeds are just not capable of taking up enough monomer to form a protrusion. However, if we measure the increase in volume of the seeds after the attempted protrusion formation we find that the increase would be sufficient to form protrusions with similar dimensions as the seeds (radius $\approx$ 150–175 nm). This indicates that the low degree of surface hydrophilicity most likely causes the lack of protrusion formation on these particles.

For the seed particles equipped with a polymeric shell consisting of 75 vol% VBC and only 25 vol% styrene we observed that with a swelling ratio of 10 (Table S2, entry 12) asymmetric dumbbells were obtained (Fig. 8d). In this case the protrusion corresponds to the larger lobe of the particle, since the two-patch particles that were present in the sample showed a very large central lobe compared to the size of the seeds. The shape of these dimers was reported previously for particles with large protrusions and is schematically depicted in Scheme 3 [1–3]. Fig. 8f and g shows TEM images of the observed dimers together with a 3D model to clarify the particle geometry. The contact angle between the seed and protrusion is not very pronounced. This can be attributed to the lower surface hydrophilicity due to the lower VBC content in the shell compared to seed particles equipped with shells of 100% p(VBC). Evidently, employing seed particles with a pure p(VBC) shell results in dumbbells with better separated lobes (Fig. 8e), but at the expense of the protrusion size (Table S1, entry 16). Naturally, this is directly coupled to the decreased swelling capability of a pure p(VBC) layer compared to the coating obtained using a mixture of 75 vol% VBC and 25 vol% styrene.

From this variation in shell composition, we conclude that a composition consisting of 75 vol% VBC and 25 vol% styrene represents the optimal balance between swelling capacity and surface hydrophilicity. Using seeds with these shells allows for the growth of protrusions with dimensions that exceed those of the employed seed particles. Deviating from this ideal shell composition yields chlorinated coatings that are either too hydrophobic to force the expelled monomer into a well-defined protrusion or too hydrophilic to accommodate enough monomer to grow protrusion of such large dimensions.

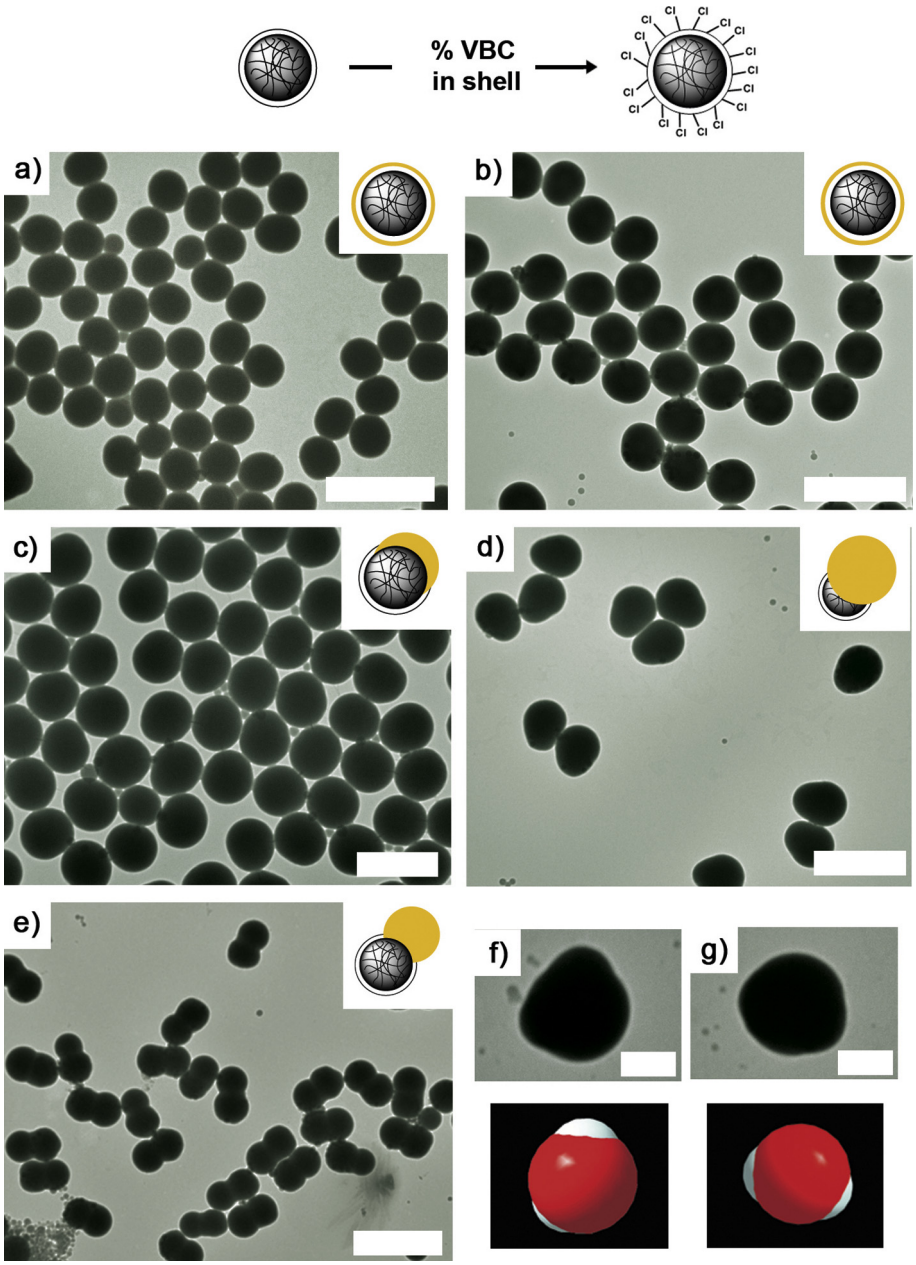

Fig. 8. Transmission electron microscopy (TEM) images of dumbbell-shaped colloids prepared by using core-shell seed particles equipped with shells grown using mixtures of styrene and 4-vinylbenzyl chloride (VBC) at swelling ratio 10. The volume percentage of VBC in the monomer mixture was equal to (a) 0%, (b) 25%, (c) 50%, (d) 75% and (e) 100%. (f) and (g) TEM image of two-patch particles present in the sample shown in panel d and corresponding 3D models to clarify the particle geometry. In the 3D model the red center resembles the fused protrusions while the chlorinated seeds are shown in white. Scale bar = 0.5 μm for panels a–e and 0.25 μm for panels f and g.

4. Conclusion

We reported the synthesis of a family of chemically anisotropic, dumbbell-shaped colloids starting from cross-linked polystyrene particles functionalized with a chlorinated outer layer (Scheme 4). Swelling these particles with monomer and subsequent phase separation of this monomer from the particles yields colloids with well-defined protrusions on their surface. The presence of the benzyl chloride moieties is key in this process, since it provides surface hydrophilicity to prevent full wetting of the expelled, hydrophobic monomer. Systematic variation of the properties of the chlorinated polystyrene seed particles as well as the conditions under which protrusion were formed provided insight in the most relevant experimental parameters to tune the geometry of the resulting anisotropic particles. Dumbbells with protrusions smaller or equal to the size of the seed particles are easily accessible by tuning experimental parameters, *e.g.*, swelling ratio and cross-link density of the seed and/or protrusion. These particle geometries are characterized by size ratios (diameter of the chlorinated seed divided by the diameter of the formed protrusion) between 0.6 and 1.

Moreover, the shell properties of the seed particles have a distinct influence on the resulting particle geometry. The protrusion size increases with increasing shell thickness, suggesting that only the cross-linked shell is actively involved in the protrusion formation. Increasing the hydrophobicity of the shell by incorporation of styrene as co-monomer results in core-shell particles in which chlorine-mediated surface hydrophilicity and swelling capacity are optimized. This enables the preparation of dumbbell-shaped

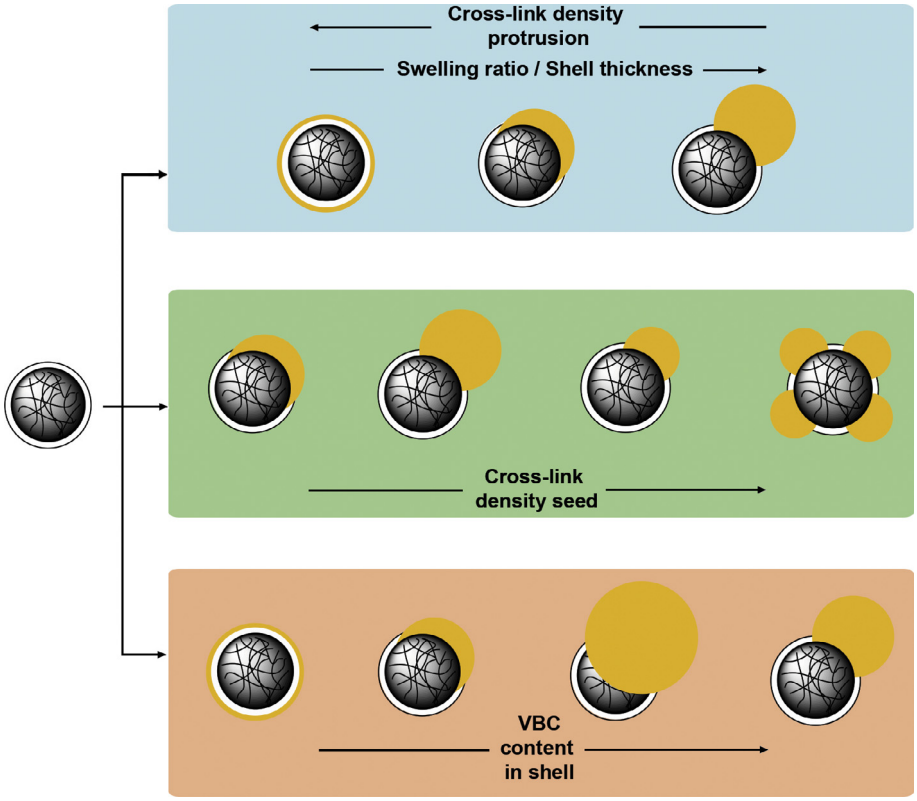

Scheme 4. Schematic overview of accessible particle geometries using chlorinated core-shell seed particles in an emulsion-based synthesis procedure to prepare anisotropic colloids. The geometries are ordered as function of the investigated experimental variables.

particles with protrusions larger than the employed seeds (size ratio = 1.4).

Besides the wide variety of particle geometries accessible via this robust synthesis route, the yield of these particles is high, since only wet-chemical, emulsion-based procedures are required. These high yields are a significant advantage compared to more complex template/surface mediated or micro-fluidic based procedures commonly employed to prepare (chemically) anisotropic colloids [38–42].

The colloids and methods to alter their geometry serve as ideal starting point for the preparation of tailored building blocks for (self-)assembly studies. By exploiting the reactivity of the chlorinated patch the preparation of directional, inter-particle interactions are within reach. The presence of chemically versatile benzyl chloride moieties is a significant advancement compared to previously reported dumbbell-shaped colloids [1,2,10,14,15,20], since it allows for exploiting a wide variety of site-specific functionalization chemistries. Following this strategy, we envision to introduce tailored molecular entities, *e.g.*, hydrophobes, polymers or supramolecular binding motives, to precisely engineer desired inter-particle potentials between the reactive lobes. Being able to tune the inter-patch interactions as well as the geometry of the building blocks paves the way to prepare novel colloidal superstructures.

Funding Sources / Acknowledgements

Antara Pal is thanked for providing the polystyrene seed particles with cross-link densities of 1 and 18%. Yong Guo is acknowledged for etching the chlorinated core-shell particles with DMF/THF and monitoring this process using TEM. Furthermore, we would like to thank the Netherlands Organization for Scientific Research (NWO) for financial support.

Appendix A. Supplementary material

Overview of all dumbbell-formation reactions. Transmission electron microscopy (TEM) images of particles obtained after varying the surfactant concentration in the reaction mixture during protrusion formation. TEM images of (dumbbell-shaped) colloids obtained using chlorinated seed particles with various cross-link densities, shell thicknesses and compositions in combination with a swelling ratio of 6. Additional TEM images of chlorinated core-shell particles after etching with DMF and THF. Comparison of dumbbell-forming ability between chlorinated seed particles with linear and cross-linked outer layers.

Supplementary data associated with this article can be found, in the online version, at http://dx.doi.org/10.1016/j.jcis.2016.11.045.

References

[1] D.J. Kraft, W.S. Vlug, C.M. van Kats, A. Van Blaaderen, A. Imhof, W.K. Kegel, Self-assembly of colloids with liquid protrusions, J. Am. Chem. Soc. 131 (2009) 1182–1186.
[2] D.J. Kraft, J. Groenewold, W.K. Kegel, Colloidal molecules with well-controlled bond angles, Soft Matter 5 (2009) 3823–3826.
[3] D.J. Kraft, J. Hilhorst, M.A.P. Heinen, M.J. Hoogenraad, B. Luigjes, W.K. Kegel, Patchy polymer colloids with tunable anisotropy dimensions, J. Phys. Chem. B 115 (2011) 7175–7181.
[4] B. Peng, H.R. Vutukuri, A. Van Blaaderen, A. Imhof, Synthesis of fluorescent monodisperse non-spherical dumbbell-like model colloids, J. Mater. Chem. 22 (2012) 21893–21900.
[5] B.G.P. Van Ravensteijn, M. Kamp, A. Van Blaaderen, W.K. Kegel, General route toward chemically anisotropic colloids, Chem. Mater. 25 (2013) 4348–4353.
[6] C. Tang, C. Zhang, J. Liu, X. Qu, J. Li, Z. Yang, Large scale synthesis of Janus submicrometer sized colloids by seeded emulsion polymerization, Macromolecules 43 (2010) 5114–5120.
[7] J.-G. Park, J.D. Forster, E.R. Dufresne, Synthesis of colloidal particles with the symmetry of water molecules, Langmuir 25 (2009) 8903–8906.
[8] J.-W. Kim, R.J. Larson, D.A. Weitz, Uniform nonspherical colloidal particles with tunable shapes, Adv. Mater. 19 (2007) 2005–2009.

[9] J.-W. Kim, J.L. Ryan, D.A. Weitz, Synthesis of nonspherical colloidal particles with anisotropic properties, J. Am. Chem. Soc. 128 (2006) 14374–14377.
[10] E.B. Mock, C.F. Zukoski, Emulsion polymerization routes to chemically anisotropic particles, Langmuir 26 (2010) 13747–13750.
[11] M. Yang, G. Wang, H. Ma, An efficient approach for production of polystyrene/poly(4-vinylpridine) particles with various morphologies based on dynamic control, Chem. Commun. 47 (2011) 911–913.
[12] J.-G. Park, J.D. Forster, E.R.J. Dufresne, High-yield synthesis of monodisperse dumbbell-shaped polymer nanoparticles, J. Am. Chem. Soc. 132 (2010) 5960–5961.
[13] W.K. Kegel, D. Breed, M. Elsesser, D.J. Pine, Formation of anisotropic polymer colloids by disparate relaxation times, Langmuir 22 (2006) 7135–7136.
[14] H.R. Sheu, M.S. El-Aasser, J.W.J. Vanderhoff, Phase separation in polystyrene latex interpenetrating polymer networks, Polym. Sci., Part A: Polym. Chem. 28 (1990) 629–651.
[15] H.R. Sheu, M.S. El-Aasser, J.W.J. Vanderhoff, Uniform nonspherical latex particles as model interpenetrating polymer networks, Polym. Sci., Part A: Polym. Chem. 28 (1990) 653–667.
[16] P.J. Flory, Thermodynamics of high polymer solutions, J. Chem. Phys. 10 (1942) 51–61.
[17] M.L. Huggins, Some properties of solutions of long-chain compounds, J. Phys. Chem. 46 (1942) 151–158.
[18] P.J. Flory, J. Rehner, Statistical mechanics of cross-linked polymer networks II. Swelling, J. Chem. Phys. 11 (1943) 521–526.
[19] M. Morton, S. Kaizerman, M.W. Altier, Swelling of latex particles, J. Colloid Sci. 9 (1954) 300–312.
[20] E.B. Mock, H. De Bruyn, B.S. Hawkett, R.G. Gilbert, C.F. Zukoski, Synthesis of anisotropic nanoparticles by seeded emulsion polymerization, Langmuir 22 (2006) 4037–4043.
[21] B.G.P. van Ravensteijn, W.K. Kegel, Versatile procedure for site-specific grafting of polymer brushes on patchy particles *via* atom transfer radical polymerization (ATRP), Polym. Chem. 7 (2016) 2858–2869.
[22] Z. Zhang, S.C. Glotzer, Self-assembly of patchy particles, Nano Lett. 4 (2004) 1407–1413.
[23] S.C. Glotzer, M.J. Solomon, N.A. Kotov, Self-assembly: from nanoscale to microscale colloids, AIChE J. 50 (2004) 2978–2985.
[24] E. Bianchi, J. Largo, P. Tartaglia, E. Zaccarelli, F. Sciortino, Phase diagram of patchy colloids: towards empty liquids, Phys. Rev. Lett. 97 (2006) 168301.
[25] F. Sciortino, A. Giacometti, G. Pastore, Numerical study of one-patch colloidal particles: from square-well to Janus, Phys. Chem. Chem. Phys. 12 (2010) 11869–11877.
[26] E. Bianchi, P. Tarlaglia, E. Zaccarelli, F. Sciortino, Theoretical and numerical study of the phase diagram of patchy colloids: ordered and disordered patch arrangements, J. Chem. Phys. 128 (2008) 144504.
[27] G. Doppelbauer, E. Bianchi, G. Kahl, Self-assembly scenarios of patchy colloidal particles in two dimensions, J. Phys.: Condens. Matter 22 (2010) 1–12.
[28] E. Mani, E. Sanz, S. Roy, M. Dijkstra, J. Groenewold, W.K. Kegel, Sheet-like assemblies of spherical particles with point-symmetrical patches, J. Chem. Phys. 136 (2012) 144706.
[29] G. Socrates, in: Infrared and Raman Characteristic Groups Frequencies, third ed., John Wiley & Sons Ltd, Chichester, England, 2001.
[30] P. van der Heide, in: X-Ray Photoelectron Spectroscopy: An Introduction to Principles and Practices, John Wiley & Sons, Inc., Hoboken, New Jersey, United States, 2012.
[31] J.C. Thomas, The determination of log normal particle size distributions by dynamic light scattering, J. Colloid Interface Sci. 117 (1987) 187–192.
[32] H. Ohshima, A simple expression for Henry's function for the retardation effect in electrophoresis of spherical colloidal particles, J. Colloid Interface Sci. 168 (1994) 269–271.
[33] W. Yang, W. Ming, J. Hu, X. Lu, S. Fu, Morphological investigations of crosslinked polystyrene microspheres by seeded polymerization, Colloid Polym. Sci. 276 (1998) 655–661.
[34] S. Baruch-Sharon, S. Margel, Preparation and characterization of core-shell polystyrene/polychloromethylstyrene and hollow polychloromethylstyrene micrometer-sized particles of narrow-size distribution, Colloid Polym. Sci. 287 (2009) 859–869.
[35] E.A. Niewenhuis, A. Vrij, Light scattering of PMMA latex particles in benzene: structural effects, J. Colloid Interface Sci. 72 (1979) 321–341.
[36] W. McPhee, K.C. Tam, R. Pelton, Poly(*N*-isopropylacrylamide) latices prepared with sodium dodecyl sulfate, J. Colloid Interface Sci. 156 (1993) 24–30.
[37] J.R. Ebdon, T.N. Huckerby, T.C. Hunter, Free-radical aqueous slurry polymerizations of acrylonitrile: 2. End-groups and other minor structures in polyacrylonitriles initiated by potassium persulfate/sodium bisulfite, Polymer 35 (1994) 4659–4664.
[38] A.B. Pawar, I. Kretzschmar, Patchy particles by glancing angle deposition, Langmuir 24 (2008) 355–358.
[39] Z. He, I. Kretzschmar, Template-assisted fabrication of patchy particles with uniform patches, Langmuir 28 (2012) 9915–9919.
[40] X.Y. Ling, I.Y. Phang, C. Acikgoz, M.D. Yilmaz, M.A. Hempenius, G.J. Vancso, J. Huskens, Janus particles with controllable patchiness and their chemical functionalization and supramolecular assembly, Angew. Chem.; Int. Ed. 48 (2009) 7677–7682.
[41] Z. Nie, W. Li, M. Seo, S. Xu, E. Kumacheva, Janus and ternary particles generated by microfluidic synthesis: design, synthesis, and self-assembly, J. Am. Chem. Soc. 128 (2006) 9408–9412.
[42] T. Nisisako, Recent advances in microfluidic production of Janus droplets and particles, Curr. Opin. Colloid Interface Sci. 25 (2016) 1–12.